A 10pJ/bit 135Mbps IR-UWB transmitter using Pulse Position Modulation and with On-chip LDO Regulator in 0.13μm CMOS for Biomedical Implants

Mohamed Elzeftawi and Luke Theogarajan

Electrical and Computer Engineering Department,
University of California Santa Barbara, Santa Barbara, CA 93106, USA.

***Abstract*— This paper describes a compact low-power high-datarate impulse radio ultra wideband (IR-UWB) transmitter IC for biomedical implants. The transmitter is powered through an on-chip low-dropout (LDO) regulator to tune its oscillation frequency which, together with the pulse width control, ensures that the transmitted pulse's power spectral density (PSD) fits within the FCC mask and has a BW $\geq 500MHz$. The transmitter uses pulse position modulation (PPM) and the maximum measured datarate is $135Mbps$ with a figure of merit of $10pJ/bit$. The chip is fabricated in $0.13\mu m$ CMOS. The core VCO occupies $(35 \times 125)\mu m^2$ area, while the area of both the regulator and the PPM oscillator is $(0.325 \times 0.17)mm^2$.**

***Index Terms*— High-datarate biotelemetry, implants, IR-UWB transmitter, LDO regulator, low-power wireless, PPM.**

I. Introduction

There has been an increasingly growing demand on low-power high-datarate transmitters for biomedical implantable electronics. For instance in brain-machine-interface (BMI), recording from several hundreds of electrodes is necessary for accurate mapping of the neural code. Several approaches has been reported including frequency-shift-keying (FSK) [1] and load-shift-keying (LSK) [2], but they suffer from low datarate that is not suitable for high density recording. Impulse radio ultra-wideband (IR-UWB) is suitable for these applications as it can support high data rates with very low power consumption for short-range communication. Most of the IR-UWB transmitters in the literature either suffer from low datarate, or poor figure of merit (FOM), or low output power, or a combination of them. In [3] the authors employed IR-UWB by generating a very narrow pulse followed by a band-pass filter to shape the output PSD to fit within the UWB's Federal Communications Commission (FCC) mask. Although $90Mbps$ datarate and good FOM were achievable, such approach suffers from small transmitted output power and thus limits the communication range. Other approaches generate multiple pulses within a specific time interval per bit to fit the output PSD within the FCC mask. However they are limited to few tens of Mbps datarate [4]-[7]. Simple robust circuits need to be designed to achieve high-datarate and yet not consume much power.

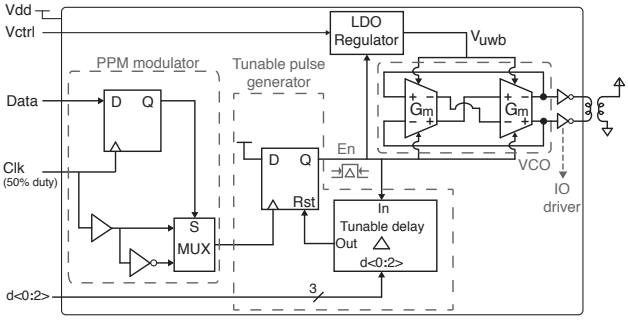

Fig. 1. Block diagram of the IR-UWB transmitter architecture using pulse positioning modulation. An on-chip LDO regulator is used to tune and power the VCO.

In this paper we present a compact low-power IR-UWB transmitter that uses pulse position modulation (PPM) and achieves measured datarate up to $135Mbps$ with a FOM of $10pJ/bit$ when transmission is centered around $3.8GHz$. The chip is fabricated in $0.13\mu m$ CMOS process. This paper is organized as follows: Section II discusses the overall IR-UWB transmitter architecture including the core voltage controlled oscillator (VCO) and low-dropout (LDO) regulator. Section III presents our wireless measurement results and summarizes our performance. Finally section IV concludes the paper.

II. IR-UWB architecture

Fig. 1 shows the block diagram of the IR-UWB transmitter. To save power, the VCO is enabled only during signal transmission. To ensure that the transmitted pulse PSD has a bandwidth $\geq 500MHz$, the time window that the oscillator needs to be enabled must be $\leq 2.5ns$, irrespective of the pulse repetition frequency (PRF). Thus a sub-nanosecond startup/shutdown oscillator is necessary in order to transmit more power within the enable window. Rapid shutdown also decreases the ringing trail after the pulse, thereby supports higher datarate, and decreases inter-symbol-interference (ISI).

The PPM modulator works as follows: The logic of the input data determines whether to trigger the tunable pulse generator at the rising (if logic "0") or falling edge (if logic

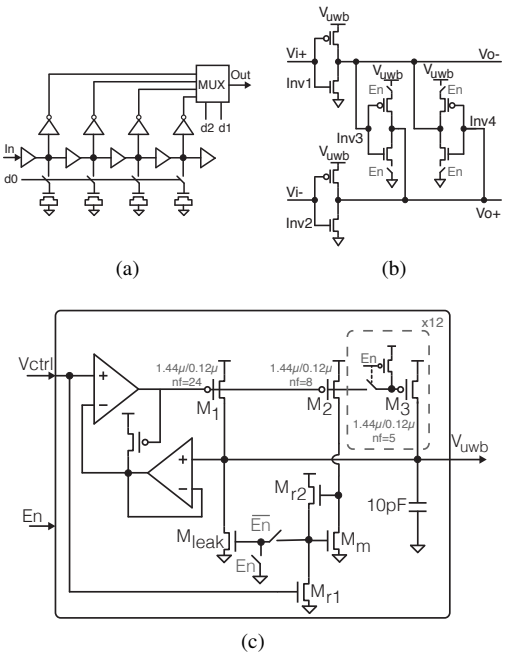

Fig. 2. (a) G_m stage using -ve resistances to speedup the startup and shutdown of the G_mC oscillator. (b) 3-bits digitally tunable delay block. (c) The LDO regulator used to power up the oscillator in pulsed mode within $\leq 2.5ns$ window.

"1") of the 50% duty-cycle clock. Once the flipflop in the tunable pulse generator is triggered, the output is asserted high, and asynchronously reset after a tunable-delay. The result is an output enable pulse, En, of width ΔT (inlcuing the Clk-Q propagation delay of the D-flipflop). The pulse width can be controlled within $1ns - 2.5ns$ through a 3-bit digitally-controlled delay block shown in Fig. 2a. This ensures that the bandwidth of the transmitted pulse will always be $\geq 500MHz$ as required by the FCC regulation. It also helps in fitting the output PSD within the FCC mask as it changes the output power transmitted per pulse. This pulse is connected to the Enable of the negative-resistances in the VCO to enable the oscillation.

The low-power G_m stage used in the VCO is a slightly modified version of Nauta's transconductance stage [8], where we removed the positive-resistance elements and only kept the negative-resistance elements as shown in Fig. 2b. At startup the En pulse enables the negative resistances (Inv3 and Inv4), which speeds-up the oscillation startup by placing the poles in the RHP. At shutdown they are disabled which speeds-up the quenching process by placing the poles in the LHP [9]. In addition to saving power, the output pulse has a raised cosine envelope which is better than a gated oscillator in terms of output harmonics.

The VCO is both tuned and powered through an on-chip LDO regulator to accommodate for process variations and to make sure the transmitted PSD lies within the FCC mask.The LDO regulator is a variation of the idea presented in [10] to make it work in pulsed mode within a

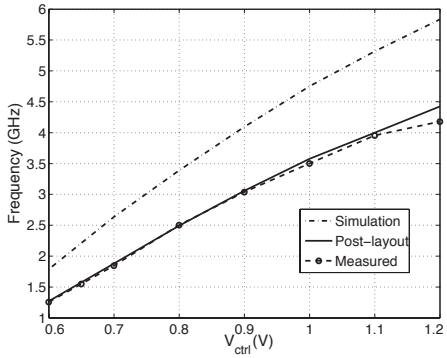

Fig. 3. Pre-, post-layout simulations, and measurement results of the regulator-powered VCO's oscillation frequency vs. V_{ctrl}.

nanosecond window as shown in Fig. 2c. The bias currents of the opamps are $Vctrl-$dependent to adapt the zero as the bias points change so that the system remains fully compensated [10]. The main regulator device, M_1, was chosen to be PMOS rather than NMOS as V_{uwb} needs to be regulated close to the supply rail. When the VCO is about to start, the 12-units of transistor M_3 get enabled to supply the large instantaneous current sinked by the VCO. They collectively provide an additional 2.5 times the current provided by M_1. Once the oscillation stops, the VCO stops sinking current and transistors M_3 are disabled to save power. M_2 and M_m mirrors one-third of M_1's current to the leak transistor, M_{leak}, to ensure that the gate voltage of M_3 and V_{uwb} stabilize at the right value before the VCO starts a new oscillation pulse.

III. Measurement Results

To test our setup, HP 70843A error performance analyzer was used to generate the clock and $(2^{15} - 1)$ pseudo-random bit sequence (PRBS) data that is fed to the IR-UWB transmitter. Rohde&Schwarz FSU50 spectrum analyzer was used to observe the output PSD and to superimpose the FCC mask. Time-domain pulses were captured by Agilent 86100C digital communication analyzer. For wireless testing, an external balun (on TX side) and single-ended antennas were used. However, a differential TX antenna can be used without requiring a balun. All measurement results were performed on leadless chip carrier (LCC84) packaged chip and using Johanson Technology's (3.1-10.3GHz) UWB chip antennas. Fig. 3 shows the pre-, post-layout simulations, and measurement results of the VCO (powered through the regulator). Layout parasitics reduced the frequency by 24%, but the measured frequency is in close agreement with the post-layout simulation.

Fig. 4a shows the received pulses' PSD for 1cm TX-RX antenna separation showing that it fits within the FCC mask which gives a feel on the maximum PSD that could be transmitted once the transmitter is in an implant. Fig. 4b shows the PSD for 12cm antenna separation showing received PSD that can be easily detected at the receiver. Fig. 5 shows the received time-domain pulses as well as

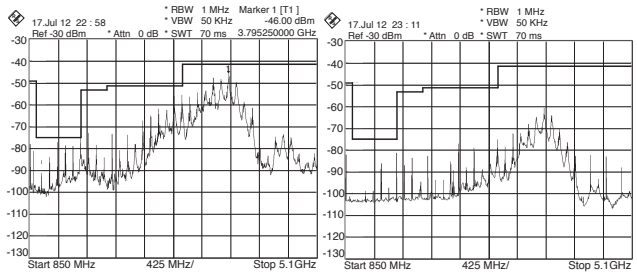

(a) (b)

Fig. 4. PSD of the wirelessly received pulses with 105MHz PRF for a TX-RX antenna separation of (a) 1cm and (b) 12cm. Both PSDs fit within the FCC mask superimposed in the figure.

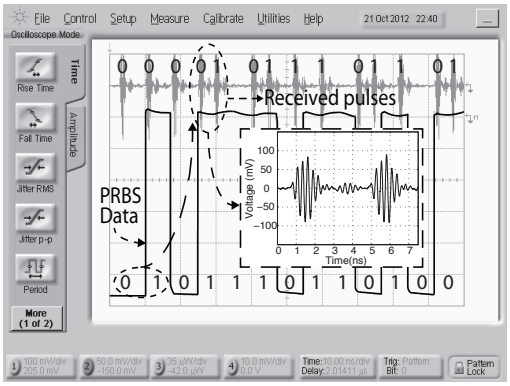

Fig. 5. Input PRBS data and the received UWB pulses with 135MHz PRF. Inset: zoom-in on the received pulses.

the PRBS data feeding the transmitter. We can see that the position of the received pulses was correctly PPM modulated at $135MHz$ PRF (at narrowest pulse width setting) and the data was successfully received. The inset shows a zoom-in on the received pulses. It is important to mention that we have set initial conditions to start the VCO in the same manner before every transmitted pulse. This is essential if a coherent receiver were to be used. However if that is not the case, these initial conditions can be removed which will add randomness in the polarity of the transmitted pulses and acts as a phase scrambler and thus decreases the spikes in the transmitted PSD.

Table I summarizes our IR-UWB transmitter performance summary and compares it to other relevant work. Our transmitter has the smallest area and highest datarate compared to all other transmitters in the table, even those fabricated in 90nm and 65nm. The achieved FOM (pJ/bit) also outperforms all the 90nm transmitters in the table.

IV. Conclusion

In this paper we presented an IR-UWB transmitter for applications demanding low-power high-datarates such as biomedical applications. Since in biomedical applications the power is usually wirelessly harvested, an on-chip regulator was used to regulate the UWB VCO's supply, isolate it from other circuits, and tune its oscillation frequency.

TABLE I
Performance Summary and Comparison to Other IR-UWB Transmitters

Metric	[3]	[4]	[5]	[6]	[7]	This work
Technology (nm)	350	90	90	90	65	130
Modulation	OOK,PPM	OOK,S-OOK	PPM+BPSK	PPM	OOK	PPM
Tunable Freq	No	Yes	Yes	Yes	Yes	Yes
Tunable pulse	No	No	Yes	No	Yes	Yes
Area (mm^2)	1	0.6*	0.07	0.08	0.7	0.055
V_{DD} (V)	±1.65	0.9	1	1	1.2	1.5
Avg. power (mW)	1.6	0.834@10MHz	4.36†	0.466@10MHz	0.2@24MHz	1.4@135MHz
Max. PRF (MHz)	90	10	15.6	16.7	24	135
FOM (pJ/bit) (@PRF)	17.7 @(90MHz)	83.4 (@10MHz)	17.5 (@15.6MHz)	47 (@10MHz)	8.5 (@24MHz)	10 (@135MHz)

* Including pads. † Power per 16-pulse-burst.

PPM modulation was used for easier synchronization at the receiver and the digitally-controlled pulse-width ensures that the transmitted PSD satisfies the FCC's mask and bandwidth requirements. The transmitter occupies only $0.055mm^2$ and capable of transmitting pulses with peak PRF of $135MHz$, yielding a FOM of $10pJ/bit$ for a transmitted PSD centered around $3.8GHz$. The achieved FOM in this $0.13\mu m$ technology outperformed other transmitters implemented in $90nm$ and the PRF outperformed transmitters implemented in both $90nm$ and $65nm$.

Acknowledgment

The authors gratefully acknowledge the support of MOSIS, especially Wes Hansford, via chip fabrication.

References

[1] L. Theogarajan, "A low-power integrated circuit for a wireless 100-electrode neural recording system," *IEEE J. of Solid-State Circuits*, vol. 42, no. 1, pp. 123–133, 2007.

[2] M. Mollazadeh, K. Murari, H. Schwerdt, X. Wang, N. Thakor, and G. Cauwenberghs, "Wireless multichannel acquisition of neuropotentials," in *Biomedical Circuits and Systems Conference, 2008. BioCAS 2008. IEEE*, nov. 2008, pp. 49 –52.

[3] M. S. Chae, Z. Yang, M. Yuce, L. Hoang, and W. Liu, "A 128-channel 6 mw wireless neural recording ic with spike feature extraction and uwb transmitter," *Neural Systems and Rehabilitation Engineering, IEEE Transactions on*, vol. 17, no. 4, pp. 312 –321, aug. 2009.

[4] M. Crepaldi, C. Li, K. Dronson, J. Fernandes, and P. Kinget, "An ultra-low-power interference-robust ir-uwb transceiver chipset using self-synchronizing ook modulation," in *IEEE International Solid-State Circuits Conference - (ISSCC)*, vol. 42, 2010, pp. 226–227.

[5] P. Mercier, D. Daly, and A. Chandrakasan, "An energy-efficient all-digital uwb transmitter employing dual capacitively-coupled pulse-shaping drivers," *IEEE Journal of Solid-State Circuits*, vol. 44, no. 6, pp. 1679–1688, 2009.

[6] D. D. Wentzloff and A. P. Chandrakasan, "A 47pj/pulse 3.1-to-5ghz all-digital uwb transmitter in 90nm cmos," in *2007 IEEE International Solid-State Circuits Conference. Digest of Technical Papers*, 2007, pp. 118–591.

[7] H. Miranda and T. Meng, "A programmable pulse uwb transmitter with 34% energy efficiency for multichannel neuro-recording systems," in *IEEE Custom Integrated Circuits Conference (CICC)*, 2010, pp. 1–4.

[8] B. Nauta and E. Seevinck, "Linear cmos transconductance element for vhf filters," *Electronics Letters*, vol. 25, no. 7, pp. 448–450, 1989.

[9] J. De Lima, "A linearly-tunable ota-c sinusoidal oscillator for low-voltage applications," in *IEEE International Symposium on Circuits and Systems (ISCAS)*, vol. 2, 2002, pp. II–408 – II–411.

[10] L. Theogarajan, "A low-power fully implantable 15-channel retinal stimulator chip," *IEEE J. of Solid-State Circuits*, vol. 43, no. 10, pp. 2322–2337, 2008.